

Coordination Chemistry of the Solvated Ag^I and Au^I Ions in Liquid and Aqueous Ammonia, Trialkyl and Triphenyl Phosphite, and Tri-*n*-butylphosphine Solutions

Kersti B. Nilsson, Ingmar Persson,* and Vadim G. Kessler

Department of Chemistry, Swedish University of Agricultural Sciences, P.O. Box 7015, SE-750 07 Uppsala, Sweden

Received January 31, 2006

The coordination chemistry of solvated Ag^I and Au^I ions has been studied in some of the most strong electron-pair donor solvents, liquid and aqueous ammonia, and the P donor solvents triethyl, tri-*n*-butyl, and triphenyl phosphite and tri-*n*-butylphosphine. The solvated Ag^I ions have been characterized in solution by means of extended X-ray absorption fine structure (EXAFS), Raman, and ¹⁰⁷Ag NMR spectroscopy and the solid solvates by means of thermogravimetry and EXAFS and Raman spectroscopy. The Ag^I ion is two- and three-coordinated in aqueous and liquid ammonia solutions with mean Ag–N bond distances of 2.15(1) and 2.26(1) Å, respectively. The crystal structure of [Ag(NH₃)₃]ClO₄·0.47 NH₃ (**1**) reveals a regular trigonal-coplanar coordination around the Ag^I ion with Ag–N bond distances of 2.263(6) Å and a Ag···Ag distance of 3.278(2) Å separating the complexes. The decomposition products of **1** have been analyzed, and one of them, [Ag(NH₃)₂]ClO₄, has been structurally characterized by means of EXAFS, showing [Ag(NH₃)₂] units connected into chains by double O bridges from perchlorate ions; the Ag···Ag distance is 3.01(1) Å. The linear bisamminegold(I) complex, [Au(NH₃)₂]⁺, is predominant in both liquid and aqueous ammonia solutions, as well as in solid [Au(NH₃)₂]BF₄, with Au–N bond distances of 2.022(5), 2.025(5), and 2.026(7) Å, respectively. The solvated Ag^I ions are three-coordinated, most probably in triangular fashion, in the P donor solvents with mean Ag–P bond distances of 2.48–2.53 Å. The Au^I ions are three-coordinated in triethyl phosphite and tri-*n*-butylphosphine solutions with mean Au–P bond distances of 2.37(1) and 2.40(1) Å, respectively.

Introduction

Ammonia is the N donor solvent possessing the strongest electron-pair donor properties, $D_S = 56$,¹ in comparison with 12 and 38 for acetonitrile and pyridine, respectively.² The Ag^I ion is regarded as a typical soft electron-pair acceptor, and very stable silver(I)–ammonia complexes are formed in aqueous solution. The formation of aminesilver(I) complexes in aqueous ammonia was studied very early.³ The stability constant of the second complex, [Ag(NH₃)₂]⁺, $\log \beta_2$, was determined soon thereafter to ca. 7.2, depending on the ionic medium and temperature,^{4,5} and Bjerrum reported

4 decades later the stepwise stability constants to $\log K_1 = 3.315$ and $\log K_2 = 3.915$.⁶ Thus, the second complex is somewhat stronger than the first one, and the bisammine-silver(I) complex is strongly dominating (>99.8%) in solutions with a free ammonia concentration of 0.01 mmol·dm⁻³ or more (calculated from the stability constants reported by Bjerrum⁶). These stability constants have been reproduced by a large number of research groups.⁷ In addition to the linear complex, Hancock and Bjerrum reported independently much later the presence of a very weak trisamminesilver(I)

* To whom correspondence should be addressed. E-mail: ingmar.persson@kemi.slu.se.

(1) Nilsson, K. B.; Maliarik, M.; Persson, I.; Sandström, M., unpublished data. New Raman data on HgI₂ in liquid ammonia reveals $\nu(\text{Hg}-\text{I}) = 132 \text{ cm}^{-1}$, giving $D_S = 56$.

(2) Sandström, M.; Persson, P.; Persson, I. *Acta Chem. Scand.* **1990**, *44*, 653.

(3) Berthelot, D.; Delepine, M. *Compt. Rend.* **1899**, *129*, 326.

(4) Bodländer, G.; Fittig, G. *Z. Phys. Chem.* **1902**, *39*, 597.

(5) von Euler, H. *Ber. Bunsen-Ges.* **1903**, *36*, 1854, 2878, 3400.

(6) Bjerrum, J. Thesis; Report 1957; P. Haase & Son: Copenhagen, Denmark, 1941.

(7) Sillén, L. G.; Martell, A. E. *Stability Constants of Metal-Ion Complexes*, Special Publication Nos. 17 and 25; The Chemical Society: London, 1964 and 1971. Pettit, L. *IUPAC Chemical Series No. 22*; IUPAC Stability Constant Database; Academic Software: Timble, Otley, Yorks, U.K., 2000, and references cited therein. Homepage: www.acadsoft.co.uk.

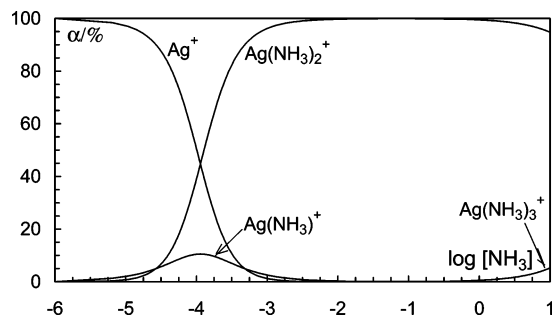


Figure 1. Complex distribution function of the silver(I)-ammonia system in water.

complex in a concentrated aqueous ammonia solution, $\log K_3 = -0.76$ and -1.60 , respectively.^{8,9} The very small stability constant of the third complex shows that it is never dominating, ca. 0.55 and 5.2% at $\log [\text{NH}_3] = 0.0$ and 1.0 , respectively, using Bjerrum's values of K_1-K_3 ^{6,9} (Figure 1).

The ammonia-solvated Cu^I ion is three-coordinated in trigonal fashion in liquid ammonia,¹⁰ with a structure very similar to that of the trisamminecopper(I) complex in the solid nitrate salt.¹¹ It can be assumed that the ammonia-solvated Ag^I ion is three-coordinated in the same way as the Cu^I ion in liquid ammonia because the Ag^I ion, as well as the Cu^I ion, forms a weak third complex in aqueous solution⁷ and the fact that the Ag^I ion in solid $[\text{Ag}(\text{NH}_3)_3]\text{NO}_3$, precipitated from liquid ammonia, has a trigonal-planar configuration. The Ag-N bond distance in solid $[\text{Ag}(\text{NH}_3)_3]\text{NO}_3$ is 2.281(7) Å.¹¹ On the other hand, a linear bisammine-silver(I) complex is expected to dominate strongly in aqueous ammonia solutions because the third complex is very weak (Figure 1). The crystal structures of $[\text{Ag}(\text{NH}_3)_2][\text{Ag}(\text{NO}_2)_2]$, $[\text{Ag}(\text{NH}_3)_2]\text{NO}_3$, $[\text{Ag}(\text{NH}_3)_2]_2\text{SO}_4$, $[\text{Ag}(\text{NH}_3)_2]\text{ClO}_4$, catena-(bis(μ_3 -hexamethylenetetraamine)disilver(I) bis(bisammine-silver(I)) 1,2,4,5,-benzenetetracarboxylate trihydrate, and bis(bisammine-silver(I) bis(biuretato-*N,N'*)nickel(II) hexahydrate all contain a linear bisammine-silver(I) complex with mean Ag-N bond distances of 2.115,¹² 2.15(2),¹¹ 2.110(3),¹³ 2.11–2.16 (two different phases at ambient and low temperature),¹⁴ 2.121,¹⁵ and 2.122 Å,¹⁶ respectively. The mean Ag-N bond distance in an aqueous ammonia solution of silver(I) nitrate, where the bisammine-silver(I) complex is strongly dominating, is reported from a large-angle X-ray scattering (LAXS) study to be 2.22(2) Å.¹⁷ This is much longer than that found for the same complex in the solid state, and it seems very doubtful that this Ag-N bond distance is correct.

Gans and Gill interpreted their Raman results of the Ag^I complex in liquid ammonia as four-coordination.¹⁸ The view

of a tetrahedrally coordinated ammonia-solvated Ag^I ion in liquid ammonia has been supported by an extended X-ray absorption fine structure (EXAFS) study, reporting a mean Ag-N bond distance of 2.31 Å.¹⁹

The structures of a number of silver(I) triphenylphosphine complexes in the solid state have been reported.^{20a} The isolated tris- and tetrakis(triarylphosphine)silver(I) complexes are trigonal, with a very slight pyramidal distortion,²¹ and tetrahedral,^{21a,22} with mean Ag-P bond distances of 2.517 (mean of 6 structures) and 2.654 Å (12 structures), respectively. Five structures containing a bis(triphenylphosphine)-silver(I) complex have been reported; the mean Ag-P bond distance is 2.411 Å.²³ To our knowledge, no structures of isolated tris- and tetrakis(trialkylphosphine)silver(I) complexes have been reported in the solid state.^{20a} Two linear bis(trialkylphosphine)silver(I) complexes, bis(trimethylphosphine)-²⁴ and bis[tris(cyanoethylphosphine)]silver(I),²⁵ with mean Ag-P bond distances of 2.377 and 2.383 Å, respectively, have been structurally characterized. This shows that the Ag-P bonds are shorter, and most probably also stronger, to trialkylphosphines than to triphenylphosphine, supported by complex formation studies.²⁶

- (8) Hancock, R. S. *Afr. J. Chem.* **1979**, 32, 49.
 (9) Bjerrum, J. *Acta Chem. Scand., Ser A* **1986**, 40, 392.
 (10) Nilsson, K. B.; Persson, I. *Dalton Trans.* **2004**, 1312 and references cited therein.
 (11) Zachwieja, U.; Jacobs, H. Z. *Anorg. Allg. Chem.* **1989**, 571, 37.
 (12) Maurer, H. M.; Weiss, A. Z. *Kristallogr.* **1977**, 146, 227.
 (13) Zachwieja, U.; Jacobs, H. Z. *Kristallogr.* **1992**, 201, 207.
 (14) Nockemann, P.; Meyer, G. Z. *Anorg. Allg. Chem.* **2002**, 628, 1636.
 (15) Zheng, S.-L.; Tong, M.-L.; Chen, X.-M.; Ng, S.-W. *J. Chem. Soc., Dalton Trans.* **2002**, 360.
 (16) Pajunen, A.; Pajunen, S. *Acta Crystallogr., Sect. C* **1994**, 50, 1884.

- (17) Maeda, M.; Maegawa, Y.; Yamaguchi, T.; Othaki, H. *Bull. Chem. Soc. Jpn.* **1979**, 52, 2545.
 (18) Gans, P.; Gill, J. B. *J. Chem. Soc., Dalton Trans.* **1976**, 779.
 (19) Yamaguchi, T.; Wakita, H.; Nomura, M. *J. Chem. Soc., Chem. Commun.* **1988**, 433.
 (20) (a) Allen, F. H.; Bellard, S.; Brice, M. D.; Cartwright, B. A.; Doubleday, A.; Higgs, H.; Hummelink, T.; Hummelink-Peters, C. G.; Kennard, O.; Motherwell, W. D. S.; Rodgers, J. R.; Watson, D. G. The Cambridge Crystallographic Data Centre: computer-based search, retrieval, analysis and display of information. *Acta Crystallogr., Sect. B* **1979**, 35, 2331 and references cited therein. (b) *Inorganic Crystal Structure Data Base*, release 04/2; National Institute of Standards and Technology, Fachinformationszentrum: Karlsruhe, Germany.
 (21) (a) Barron, P. F.; Dyason, J. C.; Healy, P. C.; Engelhardt, L. M.; Skelton, B. W.; White, A. H. *J. Chem. Soc., Dalton Trans.* **1986**, 1965. (b) Bruce, M. I.; Duffy, D. N. *Aust. J. Chem.* **1986**, 39, 1691. (c) Tiekink, E. R. T. *J. Coord. Chem.* **1993**, 28, 223. (d) Nieger, M.; Hupfer, H.; Niecke, E.; Radseck, J. Code JOBQAS in the Cambridge Structure Database. (e) Baiada, A.; Jardine, F. H.; Willett, R. D. *Inorg. Chem.* **1990**, 29, 4805. (f) Barranco, E. M.; Crespo, O.; Gimeno, M. C.; Laguna, A.; Jones, P. G.; Ahrens, B. *Inorg. Chem.* **2000**, 39, 680.
 (22) (a) Yang, S.-Y.; Xie, Z.-X.; Ng, S. W. *Acta Crystallogr., Sect. C* **2004**, 60, m123. (b) Pelizzi, C.; Pelizzi, G.; Tarasconi, P. *J. Organomet. Chem.* **1984**, 277, 29. (c) Engelhardt, L. M.; Patawachai, C.; White, A. H.; Healy, P. C. *J. Chem. Soc., Dalton Trans.* **1985**, 125. (d) Cotton, F. A.; Luck, R. L. *Acta Crystallogr., Sect. C* **1989**, 45, 1222. (e) Bowmaker, G. A.; Healy, P. C.; Engelhardt, L. M.; Kildea, J. D.; Skelton, B. W.; White, A. H. *Aust. J. Chem.* **1990**, 43, 1697. (f) Bowmaker, G. A.; Effendy, Hart, R. D.; Kildea, J. D.; de Silva, E. N.; Skelton, B. W.; White, A. H. *Aust. J. Chem.* **1990**, 50, 539. (g) Romualdo, L. L.; Bessler, K. E.; Defflon, V. M.; Niquet, E. Z. *Anorg. Allg. Chem.* **2002**, 628, 1098. (h) Del Zotto, A.; Zangrando, E. *Inorg. Chim. Acta* **1998**, 277, 111. (i) Marsh, R. E. *Acta Crystallogr., Sect. B* **2002**, 58, 893. (j) Long, D.-L.; Xin, X.-Q.; Chen, X.-M.; Kang, B.-S. *Polyhedron* **1997**, 16, 1259. (k) Ellis, D. D.; Spek, A. L. *Acta Crystallogr., Sect. C* **2000**, 56, e547.
 (23) (a) Clarke, A. J.; Ingleson, M. J.; Kociok-Kohn, G.; Mahon, M. F.; Patmore, N. J.; Pourke, J. P.; Ruggiero, G. D.; Weller, A. S. *J. Am. Chem. Soc.* **2004**, 126, 1503. (b) Thomaier, J.; Boulmaaz, S.; Schönberg, H.; Ruegger, H.; Currao, A.; Grutzmacher, H.; Hillebrecht, H.; Pritzkow, H. *New J. Chem.* **1998**, 22, 947. (c) Bowmaker, G. A.; Effendy; Reid, J. C.; Rickard, C. E. F.; Skelton, B. W.; White, A. H. *J. Chem. Soc., Dalton Trans.* **1998**, 2139. (d) Bachman, R. E.; Andretta, D. F. *Inorg. Chem.* **1998**, 37, 5657. Bayler, A.; Schier, A.; Bowmaker, G. A.; Schmidbaur, H. *J. Am. Chem. Soc.* **1996**, 118, 7006.
 (24) Alyea, E. C.; Kannan, S.; Meehan, P. R. *Acta Crystallogr., Sect. C* **2002**, 58, m365.
 (25) Liu, C. W.; Pan, H.; Fackler, J. P., Jr.; Wu, G.; Wasylishen, R. E.; Shang, M. *J. Chem. Soc., Dalton Trans.* **1995**, 3691.

Only one structure of a silver(I) triphenyl phosphite solvate complex is reported.²⁷ In this compound, bis(μ -nitrate)bis-[bis(triphenyl phosphite)silver(I)], the Ag^I ion is surrounded by two P atoms and two nitrate O atoms in a distorted tetrahedral arrangement with Ag–P bond distances of 2.402–2.404 Å and a P–Ag–P angle of 147.9°.

Au^I is only stable in solvents coordinating through N, P, or S, while in O donor solvents, Au^{III} is the most stable oxidation state. The coordination of the solvated Au^I ion in the N donor solvents pyridine and acetonitrile is assumed to be tetrahedral with mean Au–N bond distances of 2.16(2) and 2.19(2) Å, respectively,²⁸ while the Au^I solvate complexes in solvents with the softer and more polarizable P, S, and ammonia N donor atoms are linear.²⁰ Au^I forms extremely stable complexes with ammonia in aqueous solution, $\log \beta_2 = 26.5$.²⁹ The [Au(NH₃)₂]⁺ complex is most probably linear in aqueous solution, as was found in the solid [Au(NH₃)₂]Br salt, with Au–N bond distances of 2.01(2)–2.03(2) Å.³⁰ Several bisamminegold(I) complexes have been synthesized, but the structural information is limited.^{30,31}

The structures of the isolated bis-, tris-, and tetrakis-(triphenylphosphine)gold(I) complexes in the solid state are linear,³² trigonal,³³ and tetrahedral^{33a,34} with mean Ag–P bond distances of 2.312, 2.387, and 2.634 Å, respectively. The structures of a large number of linear bis(trialkylphosphine)-gold(I) complexes are reported,^{20a} with a mean Au–P bond distance of 2.309 Å, while no structure has been reported for any tris(trialkylphosphine)gold(I) complex. The structures of four tetrakis(1,3,5-triaza-7-phosphaadamantane)gold(I) complexes have a surprisingly short mean Au–P bond distance, 2.397 Å.³⁵ The mean Au–P bond distances are the same for

the bis(trialkylphosphine)- and bis(triphenylphosphine)gold(I) complexes and for the tris(trialkylphosphine)-³⁶ and tris-(triphenylphosphine)gold(I) complexes, respectively. The surprisingly large difference in the Au–P bond distance between tris- and tetrakis(triphenylphosphine)gold(I) complexes is probably caused by steric hindrance in the latter.

The aim of this study is to describe the coordination chemistry of the Ag^I and Au^I ions in some of the strongest electron-pair donor solvents known, ammonia and P donor solvents.^{1,2} 1:1 salts of monovalent metal ions are the only ones that can be dissolved and dissociated in P donor solvents; the low permittivity of these solvents prevents dissociation of salts containing di- or trivalent ions. The structure of the solvated Cu^I ion in strong electron-pair donor solvents displays frequently a lower coordination number than is geometrically allowed because of the soft bonding character of both the metal ion and solvent.¹⁰ This paper reports the coordination chemistry of the even softer Ag^I and Au^I ions as a continuation of the Cu^I study. A literature survey of ammonia-, phosphite-, and phosphine-solvated Cu^I, Ag^I, and Au^I ions in the solid state and the results in the present study in solution describe the coordination chemistry in these very strong electron-pair acceptor–donor systems. The structural studies in solution are performed with EXAFS, and a crystallographic determination of solid [Ag(NH₃)₃]ClO₄·0.47NH₃ is reported as well.¹⁰⁷ Ag NMR and Raman spectroscopy and thermogravimetric analysis (TGA) measurements are reported to further characterize the complexes synthesized and/or structurally characterized in solution.

Experimental Section

Solvents. Liquid ammonia was distilled from 25% aqueous ammonia (analytical grade, Merck) and used within some hours. The distillation procedure has been described in detail elsewhere.¹⁶ Trialkyl and triphenyl phosphites and tri-*n*-butylphosphine (reagent grade, Sigma-Aldrich) were used without further purification.

Chemicals and Preparation of Solutions. Solid trisammine-silver(I) perchlorate, [Ag(NH₃)₃]ClO₄·0.47 NH₃ (**1**), was prepared by dissolving anhydrous silver perchlorate in liquid ammonia at ca. 220 K, and the temperature was slowly elevated to boil off the ammonia. The white crystals formed were recrystallized once from liquid ammonia before crystallographic examination. This compound is very unstable outside the mother-liquid or ammonia atmosphere and was stored in a refrigerator in an ammonia atmosphere prior to analysis. The grinding of these crystals in order to perform a homogeneous mixture with boron nitride (BN) for EXAFS measurements caused a rapid decomposition to bisammine-silver(I) perchlorate, [Ag(NH₃)₂]ClO₄ (**2**). When the mixture was heated to 433 K, a further decrease of the ammonia content occurred and monoammine-silver(I) perchlorate, Ag(NH₃)ClO₄, was formed. Anhydrous silver(I) nitrate, AgNO₃ (Fluka), and silver(I) chloride, AgCl (Fluka), were dried in an oven before use.

Solid bisamminegold(I) tetrafluoroborate, [Au(NH₃)₂]BF₄ (**3**), was prepared by dissolving ca. 0.5 g of metallic Au powder (99.9%, Aldrich) in a 100-cm³ dry acetonitrile solution of nitrosyl tetrafluoroborate, NOBF₄ (Merck), ca. 0.5 g, at room temperature as

- (26) (a) Ahrland, S.; Hultén, F.; Persson, I. *Acta Chem. Scand., Ser. A* **1986**, *40*, 595. (b) Hultén, F.; Persson, I. *Inorg. Chim. Acta* **1987**, *128*, 43.
- (27) Ahlgren, M.; Pakkanen, T.; Tahvainen, I. *Acta Chem. Scand., Ser. A* **1985**, *39*, 651.
- (28) Ahrland, S.; Nilsson, K.; Persson, I.; Yuchi, A.; Penner-Hahn, J. E. *Inorg. Chem.* **1989**, *28*, 1833.
- (29) Skibsted, L.; Bjerrum, J. *Acta Chem. Scand., Ser. A* **1974**, *28*, 740, 764.
- (30) Mingos, D. M. P.; Yau, J.; Menzer, S.; Williams, D. J. *J. Chem. Soc., Dalton Trans.* **1995**, 319.
- (31) Vicente, J.; Chicote, M.; Guerrero, R.; Jones, P. G.; Ramírez de Arellano, M. *Inorg. Chem.* **1997**, *36*, 4438.
- (32) (a) Bruce, M. I.; Walton, J. K.; Skelton, B. W.; White, A. H. *J. Chem. Soc., Dalton Trans.* **1983**, 809. (b) Baenziger, N. C.; Bennett, W. E.; Soboroff, D. M.; O'Donnell, P. S.; Doyle, J. R. *Polyhedron* **1998**, *17*, 2379. (c) Baukova, T. V.; Kravtsov, D. N.; Kuz'mina, L. G.; Dvortsova, N. V.; Porai-Koshits, M. A.; Perevalova, E. G. *J. Organomet. Chem.* **1989**, *465*, 372. (d) Baukova, T. V.; Ellert, O. G.; Kuz'mina, L. G.; Dvortsova, N. V.; Lemenovskii, D. A.; Rubezhov, A. Z. *Mendeleev Commun.* **1991**, 22. (e) Staples, R. J.; King, C.; Khan, M. N. I.; Winpenny, R. E. P.; Fackler, J. P., Jr. *Acta Crystallogr., Sect. C* **1993**, *49*, 472. (f) Alonso, P. J.; Cerrada, E.; Garin, J.; Gimeno, M. C.; Laguna, A.; Laguna, M.; Jones, P. G. *Synth. Met.* **1993**, *55*, 1772. (g) Marsch, R. E.; Spek, A. L. *Acta Crystallogr., Sect. B* **2001**, *57*, 800. (h) Anderson, S.; Mullica, D. F.; Sappenfield, E. L.; Stone, F. G. A. *Organometallics* **1995**, *14*, 3516. (i) Wang, J.-C. *Acta Crystallogr., Sect. C* **1996**, *52*, 611.
- (33) (a) Jones, P. G. *Chem. Commun.* **1980**, 1031. (b) Beurskens, P. T.; Pet, R.; Noordik, J. H.; Van der Velden, J. W. A.; Bour, J. J. *Cryst. Struct. Commun.* **1982**, *11*, 1039. (c) Hamel, A.; Schier, A.; Schmid-baur, H. Z. *Naturforsch., Teil B* **2002**, *57*, 877. (d) Davidson, J. L.; Lindsell, W. E.; McCullough, K. J.; McIntosh, C. H. *Organometallics* **1995**, *14*, 3497. (e) Olbrich, F.; Lagow, R. J. *Z. Anorg. Allg. Chem.* **1995**, *621*, 1929.
- (34) Lansun, Z.; Huahui, Y.; Wenbing, Y.; Qianer, Z. *Z. Xiamen Daxue Xuebao, Ziran Kexueban* **1990**, *29*, 421.

(35) Forward, J. M.; Assefa, Z.; Staples, R. J.; Fackler, J. P. *Inorg. Chem.* **1996**, *35*, 16.

(36) McCleskey, T. M.; Henling, L. M.; Flanagan, K. A.; Gray, H. B. *Acta Crystallogr., Sect. C* **1993**, *49*, 1467.

Table 1. Compositions of the Studied Solutions

sample	concentration/ mol·dm ⁻³	method ^a
AgCl in NH ₃ (aq)	0.7	E
AgNO ₃ in NH ₃ (aq)	2.0	R
AgClO ₄ in NH ₃ (l)	0.6	E, R
AgNO ₃ in NH ₃ (l)	0.44	R
AgNO ₃ in Me ₂ NCHS	0.5	N
AgClO ₄ in P(OCH ₃) ₃	0.5	N
AgClO ₄ in P(OC ₂ H ₅) ₃	0.7	E
AgClO ₄ in P(OC ₄ H ₉) ₃	0.61	E
AgClO ₄ in P(OC ₆ H ₅) ₃	0.15	E
AgClO ₄ in P(C ₄ H ₉) ₃	0.5	E, N
[Au(NH ₃) ₂]BF ₄ in NH ₃ (aq)	0.6	E
[Au(NH ₃) ₂]BF ₄ in NH ₃ (l)	sat. sol./0.6	E, R
AuBF ₄ in P(OC ₂ H ₅) ₃	0.35	E

^a N = ¹⁰⁷Ag NMR, E = EXAFS, L = LAXS, and R = Raman spectroscopy.

described elsewhere.³⁷ The volume of this solution was reduced to ca. 10 cm³ and mixed with freshly distilled water-free liquid ammonia. When the liquid ammonia had evaporated, yellow crystals of **3** were formed. It is important to stress that all chemicals must be very dry during the synthesis; otherwise, a black precipitate is immediately formed. Weighed amounts of **3** were dissolved in the solvents studied; the prepared [Au(NH₃)₂]⁺ complexes are perfectly stable in aqueous systems.

The concentrations of the studied solutions are summarized in Table 1.

EXAFS: Data Collection. Ag K-edge and Au L_{III}-edge X-ray absorption spectra were recorded at the wiggler beam line 4-1 at the Stanford Synchrotron Radiation Laboratory (SSRL). The EXAFS station was equipped with a Si[220] double-crystal monochromator. SSRL operated at 3.0 GeV and a maximum current of 100 mA. The data collections were performed in transmission mode, except for Au^I in aqueous ammonia and tri-*n*-butylphosphine solutions, where fluorescence mode, using a Lytle detector with a flow of Ar, was applied. The experiments were performed at ambient temperature, except for the measurement of the Au^I solvate in a liquid ammonia solution, when the temperature of the sample was kept at about 200 K. Higher order harmonics were reduced by detuning the second monochromator to 70 and 50% of the maximum intensity at the end of the scans for Ag and Au, respectively. The solid compounds were diluted in BN to give an edge step of about one unit in the logarithmic intensity ratio and kept in sample cells made of 1-mm brass frames with Mylar tape windows. The phosphite and phosphine solutions of Ag^I and Au^I were measured in sample cells with 1.5–2-mm Vitone spacers and 35–55-μm glass windows. The liquid and aqueous ammonia solutions of silver(I) perchlorate were kept in 1.5-mL airtight glass vials with an outer diameter of ca. 10 mm. The liquid ammonia solution of Au^I was contained in a 2-mm Ti spacer with 35–55-μm glass windows, equipped with a Cu rod, which was dipped into a methanol/liquid N₂ cooling mixture of ca. 175 K as described elsewhere.¹⁰ The temperature was slowly increasing during the experiment because of evaporation of the liquid N₂. The energy scales of the X-ray absorption spectra were calibrated by assigning the first inflection point of the K edge of a Ag foil to 25 514 eV and that of the L_{III} edge of a Au foil to 11 919 eV.³⁸ For each

(37) Bergerhoff, G. Z. *Anorg. Allg. Chem.* **1964**, 327, 139.

(38) Thompson, A.; Attwood, D.; Gullikson, E.; Howells, M.; Kim, K.-J.; Kirz, J.; Kortright, J.; Lindau, I.; Pianatta, P.; Robinson, A.; Scofield, J.; Underwood, J.; Vaughan, D.; Williams, G.; Winick, H. *X-ray Data Booklet*; LBNL/PUB-490 Revision 2; Lawrence Berkeley National Laboratory: Berkeley, CA, 2001.

Table 2. Crystallographic Data for **1** at 295 K

compound	[Ag(NH ₃) ₃]ClO ₄ ·0.47NH ₃
empirical formula	H _{10.41} ClN _{3.47} O ₄ Ag
fw	266.415
cryst size/mm	0.20 × 0.25 × 0.40
wavelength/Å	0.710 73
cryst syst	hexagonal
space group	P $\bar{3}1c$ (No. 163)
<i>a</i> /Å	8.237(3)
<i>c</i> /Å	6.555(3)
<i>V</i> /Å ³	385.1(3)
<i>Z</i>	2
<i>D_c</i> /g·cm ⁻³	2.375
<i>μ</i> (Mo Kα)/mm ⁻¹	2.936
abs corr	empirical method
transmission factors	0.384, 0.5913
<i>F</i> (000)	272
<i>θ</i> _{max} /deg	24.96
<i>h, k, l</i>	±9, -9 - +7, ±7
indep reflns	214
reflns with <i>I</i> > 2σ(<i>I</i>)	156
<i>R</i> _{int} /%	3.99
completeness (%) to <i>θ</i> = 24.96°	91.5
refinement method	full-matrix least squares on <i>F</i> ²
data/restraints/param	214/19/32
GOF on <i>F</i> ²	1.174
final <i>R</i> indices (<i>λ</i> > 2σ) ^a	<i>R</i> 1 = 0.0339 <i>wR</i> 2 = 0.0809
<i>R</i> indices (all data) ^a	<i>R</i> 1 = 0.01175 <i>wR</i> 2 = 0.0857
extinction coeff	1.2(2)
largest diff peak and hole/e·Å ⁻³	+0.238 to -0.190

^a Definition of *R* (SHELXTL): $R = \sum ||F_o| - |F_c|| / \sum |F_o|$; $R_w = [\sum (w|F_o| - |F_c|)^2 / \sum (w|F_o|)^2]^{1/2}$; $R1 = \sum ||F_o| - |F_c|| / \sum |F_o|$; $wR2 = (\sum [w(F_o^2 - F_c^2)^2] / \sum [w(F_o^2)^2])^{1/2}$.

sample, 3–6 scans were averaged. The EXAFSPAK³⁹ program package was used for the primary data treatment.

EXAFS: Data Analysis. The data analyses were performed by means of the GNXAS code in order to get the best possible splines. The GNXAS code is based on the calculation of the EXAFS signal and a subsequent refinement of the structural parameters.^{40,41} The GNXAS method accounts for multiple scattering (MS) paths, with correct treatment of the configurational average of all of the MS signals to allow fitting of correlated distances and bond distance variances (Debye–Waller factors). A correct description of the first coordination sphere of the studied complex has to account for asymmetry in the distribution of the ion–solvent distances.^{42,43} Therefore, the Ag–N and Au–N two-body signals associated with the first coordination shells were modeled with Γ-like distribution functions, which depend on four parameters, namely, the coordination number *N*, the average distance *R*, the mean-square variation σ , and the skewness β . The β term is related to the third cumulant *C*₃ through the relation $C_3 = \sigma^3\beta$, and *R* is the first moment of the function $4\pi \int g(r)^2 dr$. It is important to stress that *R* is the average distance and not the position of the maximum of the distribution (*R*_m).

The standard deviations given for the refined parameters in Tables 3 and 4 are obtained from *k*²-weighted least-squares refinements of the EXAFS function $\chi(k)$ and do not include systematic errors of the measurements. These statistical error

(39) George, G. N.; Pickering, I. J. *EXAFSPAK—A Suite of Computer Programs for Analysis of X-ray Absorption Spectra*; SSRL: Stanford, CA, 1993.

(40) Filipponi, A.; Di Cicco, A.; Natoli, C. R. *Phys. Rev. B* **1995**, 52, 15122.

(41) Filipponi, A.; Di Cicco, A. *Phys. Rev. B* **1995**, 52, 15135.

(42) Filipponi, A. *J. Phys.: Condens. Matter* **1994**, 6, 8415.

(43) Hedin, L.; Lundqvist, B. I. *J. Phys. C: Solid State Phys.* **1971**, 4, 2064.

Table 3. Mean Bond Distances, $d/\text{\AA}$, Number of Distances, N , Debye–Waller Factor Coefficients, $\sigma^2/\text{\AA}^2$, Third Cumulant Factors Describing the Asymmetry, Bond Angles Calculated from MS Pathways, θ/deg , $C_3 = \beta\sigma^3/\text{\AA}^3$, the Amplitude Reduction Factor, S_o^2 , the Threshold Energy, E_o/eV , and the Least-squares Value of the Refinement, F , of the Ammonia, Trialkyl and Triphenyl Phosphite, and Tri-*n*-butylphosphine Solvated Ag^1 Ions in Solution and the Solids $[\text{Ag}(\text{NH}_3)_2]\text{ClO}_4$ and $[\text{Ag}(\text{P}(\text{OC}_6\text{H}_5)_3)_3]\text{ClO}_4$ As Determined by EXAFS at Room Temperature

sample	scattering path	N	d	σ^2	θ	C_3	S_o^2	E_o	F
$[\text{Ag}(\text{NH}_3)_2]^+$ in $\text{NH}_3(\text{aq})$ room temperature	Ag–N	2	2.148(2)	0.0013(2)		5.6×10^{-6}	0.855	25 519.2	4.7×10^{-9}
	Ag···H	6	2.67(2)	0.0092(2)		1.3×10^{-5}			
	$\angle\text{Ag–N–H}$	6			109.6(1.0)				
$[\text{Ag}(\text{NH}_3)_3]^+$ in $\text{NH}_3(\text{l})$ room temperature	Ag–N	3	2.265(5)	0.0145(8)		4.8×10^{-6}	0.835	25 519.3	1.8×10^{-8}
	Ag–O	1	2.88(2)	0.015(2)		1.1×10^{-5}			
	$\angle\text{N–Ag–N}$	3			120.0(0.8)				
$[\text{Ag}(\text{NH}_3)_2]\text{ClO}_4(\text{s})$ (heated to 333 K, s1)	Ag–N	2	2.150(5)	0.0122(7)		3.6×10^{-6}	0.875	25 519.6	1.7×10^{-7}
	Ag–Ag	2	3.015(4)	0.0038(4)		6.2×10^{-5}			
	Ag–Ag	2	6.021(10)	0.0120(10)		0			
	Ag–O	2	3.20(3)	0.055(4)		1.5×10^{-5}			
$[\text{Ag}(\text{NH}_3)_2]\text{ClO}_4(\text{s})$ (ground at RT, s2)	Ag–N	2	2.151(5)	0.0120(7)		3.5×10^{-6}	0.877	25 519.6	1.7×10^{-7}
	Ag–Ag	2	3.012(4)	0.0038(4)		6.0×10^{-5}			
	Ag–Ag	2	6.015(10)	0.0115(10)		0			
	Ag–O	2	3.21(3)	0.054(4)		1.5×10^{-5}			
$[\text{Ag}(\text{P}(\text{OC}_2\text{H}_5)_3)_3]^+$ room temperature	Ag–P	3	2.483(3)	0.0058(2)		1.1×10^{-5}	0.885	25 517.7	1.7×10^{-7}
	Ag–O	1	2.74(3)	0.0042(4)		1.4×10^{-5}			
	P–O	9	1.385(3)	0.015(2)		2.1×10^{-6}			
	$\angle\text{Ag–P–O}$	9	3.32(2)	0.053(4)	115.4(1.4)				
	$\angle\text{P–Ag–P}$	3	4.32(2)	0.0116(6)	121.0(1.0)				
$[\text{Ag}(\text{P}(\text{OC}_4\text{H}_9)_3)_3]^+$ room temperature	Ag–P	3	2.513(2)	0.0079(2)		4.0×10^{-5}	0.915	25 517.5	7.1×10^{-8}
	Ag–O	1	2.90(4)	0.0113(5)		5.4×10^{-5}			
	P–O	9	1.380(3)	0.015(2)		3.2×10^{-6}			
	$\angle\text{Ag–P–O}$	9	3.29(2)	0.053(4)	112.1(1.4)				
	$\angle\text{P–Ag–P}$	3	4.32(2)	0.0264(5)	119.5(1.0)				
$[\text{Ag}(\text{P}(\text{OC}_6\text{H}_5)_3)_3]^+$ room temperature	Ag–P	3	2.485(2)	0.0117(3)		8.2×10^{-5}	0.874	25 518.3	1.1×10^{-7}
	Ag–O	1	2.88(3)	0.030(5)		5.2×10^{-5}			
	P–O	9	1.417(3)	0.0098(4)		1.6×10^{-6}			
	$\angle\text{Ag–P–O}$	9	3.34(2)	0.042(4)	115.4(1.0)				
$[\text{Ag}(\text{P}(\text{OC}_6\text{H}_5)_3)_3]\text{ClO}_4(\text{s})$ room temperature	Ag–P	3	2.495(2)	0.0071(2)		5.2×10^{-5}	0.886	25 518.2	1.4×10^{-7}
	P–O	9	1.380(5)	0.0140(6)		3.3×10^{-6}			
	$\angle\text{Ag–P–O}$	9	3.35(2)	0.032(3)	116.6(1.7)				
	$\angle\text{P–Ag–P}$	3	4.32(2)	0.011(1)	119.9(1.1)				
$[\text{Ag}(\text{P}(\text{C}_4\text{H}_9)_3)_3]^+$ room temperature	Ag–P	3	2.528(4)	0.0020(2)		3.7×10^{-6}	0.896	25 516.2	3.8×10^{-7}
	P–C	9	1.805(3)	0.0126(3)		4.5×10^{-6}			
	Ag–O	9	2.76(3)	0.022(4)		4.3×10^{-5}			
	$\angle\text{Ag–P–C}$	9	3.58(1)	0.0050(5)	110.3(8)				
	$\angle\text{P–Ag–P}$	3	4.46(2)	0.017(1)	123.9(1.2)				

Table 4. Mean Bond Distances, $d/\text{\AA}$, Number of Distances, N , Debye–Waller Factor Coefficients, $\sigma^2/\text{\AA}^2$, Third Cumulant Factors Describing the Asymmetry, $C_3 = \beta\sigma^3/\text{\AA}^3$, the Amplitude Reduction Factor, S_o^2 , the Threshold Energy, E_o/eV , and the Least-Squares Value of the Refinement, F , of the Ammonia, Triethyl Phosphite, and Tri-*n*-butylphosphine Solvated Au^1 Ions in Solution and Solid $[\text{Au}(\text{NH}_3)_2]\text{BF}_4$ As Determined by EXAFS^a

sample	scattering path	N	d	σ^2	θ	C_3	S_o^2	E_o	F
$[\text{Au}(\text{NH}_3)_2]^+$ in $\text{NH}_3(\text{aq})$ room temperature	Au–N	2	2.022(2)	0.0026(2)		0	0.813	11 922.2	2.1×10^{-8}
	N–H	6	1.095(5)	0.0038(3)		2.8×10^{-6}			
	$\angle\text{Au–N–H}$	6			109.9(1)				
	$\angle\text{N–Au–N}$	1			180.1(1)				
$[\text{Au}(\text{NH}_3)_2]^+$ in $\text{NH}_3(\text{l})$ ca. 200 K	Au–N	2	2.026(3)	0.0019(2)		0	0.839	11 922.3	8.1×10^{-7}
	Au–H	6	2.58(2)	0.005(2)		0			
	$\angle\text{N–Au–N}$	1			180.0(1)				
$[\text{Au}(\text{NH}_3)_2]\text{BF}_4(\text{s})$ room temperature	Au–N	2	2.025(2)	0.0032(2)		0	0.829	11 922.2	2.1×10^{-8}
	N–H	6	1.087(5)	0.0018(3)		2.1×10^{-6}			
	$\angle\text{Au–N–H}$	6			113(1)				
	$\angle\text{N–Au–N}$	1			180.0(1)				
$[\text{Au}(\text{P}(\text{OC}_2\text{H}_5)_3)_3]^+$ room temperature	Au–P	3	2.367(3)	0.0073(4)		3.2×10^{-5}	0.835	11 922.4	8.1×10^{-8}
	P–O	9	1.383(4)	0.0040(4)		5.3×10^{-6}			
	$\angle\text{Au–P–O}$	9			115.3(9)				
	$\angle\text{P–Ag–P}$	3			124.5(8)				
$[\text{Au}(\text{P}(\text{C}_4\text{H}_9)_3)_3]^+$ room temperature	Au–P	3	2.399(3)	0.0082(4)		6.5×10^{-5}	0.802	11 921.6	3.2×10^{-8}
	P–C	9	1.895(5)	0.0082(6)		4.2×10^{-6}			
	$\angle\text{Au–P–C}$	9			115.5(8)				
	$\angle\text{P–Au–P}$	3			120.8(0.5)				

^a At the presence of asymmetry, the position of the peak maximum, $R_m/\text{\AA}$, has been calculated.

estimates provide a measure of the precision of the results and allow reasonable comparisons, e.g., of the significance of relative shifts

in the distances. However, the variations in the refined parameters, including the shift in the E_o value (for which $k = 0$), using different

models and data ranges, indicate that the absolute accuracy of the distances given for the separate complexes is within ± 0.01 – 0.02 Å for well-defined interactions. The “standard deviations” given in the text have been increased accordingly to include estimated additional effects of systematic errors.

Single-Crystal X-ray Diffraction. Data were collected with a Bruker SMART CCD 1 k diffractometer at 295 ± 1 K.⁴⁴ The structure was solved by standard direct methods in the *SHELXTL* program package⁴⁵ and refined by full-matrix least squares isotropically on F^2 and finally in anisotropic approximation. H atoms were detected in difference Fourier syntheses and refined using a riding model. All calculations were performed with the *SHELXTL* programs in PC version (version 5.3).⁴⁵ Selected crystal and experimental data are summarized in Table 2. The atomic coordinates and bond distances and angles are available as CIFs in the Supporting Information.

Raman Spectroscopy. Raman spectra of the samples were measured by means of a Fourier transform (FT)-Raman module FRA106/S in combination with a Bruker IFS66/S FT-IR spectrometer equipped with a FT-Raman accessory. The 1064-nm line from a Nd:YAG laser was used to irradiate the samples, and 10–200 scans were collected at a spectral bandwidth of 2–4 cm^{-1} .

Thermogravimetry. TGA studies were performed on a Perkin-Elmer TGA7. The amount of sample used in each experiment was 5–7 mg, and heating was performed in an open Pt crucible at a rate of 10 $\text{K}\cdot\text{min}^{-1}$ in an Ar atmosphere in the range 293–873 K and in a N_2 atmosphere in the range 293–673 K.

Atomic Absorption Spectrophotometry (AAS). The Ag content in degraded **1** was determined by dissolving the samples in 5% HNO_3 and analyzing the solution using AAS on a Perkin-Elmer AAnalyst 100.

¹⁰⁷Ag and ¹⁰⁹Ag NMR Spectroscopy. The ¹⁰⁷Ag and ¹⁰⁹Ag NMR spectra were recorded at 16.20 and 18.62 MHz, respectively, on a Bruker 400 DRX spectrometer equipped with a multinuclear BBO probe. Because the chemical shift is dependent on both the anion and concentration, the results are given relative to an infinite D_2O solution of Ag^+ .⁴⁶ The spectral width was 16 234–32 467 Hz, and the number of data points in each data acquisition was 131 000. A pulse width of 6 μs (90° pulse) was used, with a recycle delay of 32 s, and the number of scans was 16–64 for samples with high concentration and 1900–7400 for samples with low concentration. The samples were kept in cylindrical tubes with an outer diameter of 5 mm at 303 K. The liquid ammonia solutions of silver perchlorate and nitrate were prepared at 220 K and then transferred into airtight 5-mm NMR tubes, Wilmad, kept under pressure. 10% CD_3CN or D_2O was used as a lock signal.

Results and Discussion

Crystal Structure of **1.** The space groups $P\bar{3}1c$ and $P6_3/mmc$ were considered for the solution and refinement for the structure of **1** on the basis of extinction analysis. The total distribution of intensities in the experiment was, however, in favor of space group $P\bar{3}1c$, as well as the extinctions, leading the $P\bar{3}1c$ space group to have markedly lower R factors compared to the $P6_3/mmc$ group. Application of the higher symmetry $P6_3/mmc$ group was, in addition, not permitting a proper placement of the additional ammonia

present in the crystal lattice. The final model presented in this paper was therefore refined in the group $P\bar{3}1c$. Selected crystallographic data and details of structural refinement are given in Table 2. The determination of the structure of the solid solvate of silver perchlorate, crystallized from liquid ammonia, **1**, reveals a regular trigonal-coplanar coordination, $\angle\text{N}-\text{Ag}-\text{N} = 120^\circ$, around the Ag^+ ion with a $\text{Ag}-\text{N}$ bond distance of 2.263(6) Å (CIF file in the Supporting Information). The Ag complexes are arranged in linear chains with a fairly short $\text{Ag}\cdots\text{Ag}$ distance in a manner almost identical with that previously reported in the corresponding nitrate salt¹⁷ (Figure 2). The $\text{Ag}\cdots\text{Ag}$ distance in **1**, 3.278(2) Å, is slightly longer than that in the nitrate salt, probably because of the presence of the larger and more spacious perchlorate anion, while the $\text{Ag}-\text{N}$ bond distances in the two compounds are similar. The four H atoms on the ammonia N atoms are due to symmetric restrictions and thereby have the occupancy of $3/4$. The intrachain metal–metal distances are caused by H bonds and not by bonding interactions between the Ag^+ ions, as concluded by Zachwieja and Jacobs in the case of the nitrate salt.¹¹ The perchlorate anions are severely disordered. The structure contains partially occupied ammonia positions in the potentially empty spaces occurring as a result of the presence of the comparably large perchlorate anions. This may explain the assumption made by Gans and Gill of the formation of the compound with the empirical formula $[\text{Ag}(\text{NH}_3)_4]\text{ClO}_4$.¹⁸

Degradation Products of **1.** When **1** was heated to 333 K for 10 min or ground in a mortar prior to the EXAFS analysis, the structure did decompose to essentially $[\text{Ag}(\text{NH}_3)_2]\text{ClO}_4$. The EXAFS data analyses showed the presence of a $\text{Ag}-\text{N}$ bond distance of 2.15(1) Å, typical for a linear complex (see above), and a short $\text{Ag}\cdots\text{Ag}$ distance of 3.012–(10) Å, in both samples (Table 3 and Figure 3). The XANES spectra show a distinct shoulder on the edge typical for linear Ag complexes (Figure S1 in the Supporting Information). The solid-state structures of two modifications of $[\text{Ag}(\text{NH}_3)_2]\text{ClO}_4$ have been reported with transition temperatures at 200–210 K; the $\text{Ag}\cdots\text{Ag}$ distances in the low- and high-temperature phases are 3.020 and 3.0885 Å, respectively.¹⁴ Thus, the $\text{Ag}\cdots\text{Ag}$ distance in the decomposition products is very similar to that observed in the low-temperature phase. When the same sample was ground and heated to 433 K for 10 min, the product was essentially $[\text{Ag}(\text{NH}_3)]\text{ClO}_4$, with a Ag content of 48.8% (expt), 48.1% (theor). No structure determination of $[\text{Ag}(\text{NH}_3)]\text{ClO}_4$ was performed. The fit of the EXAFS data is given in Figure 3 and that of the Fourier transforms in Figure S2 in the Supporting Information.

TGAs were performed on the crystals of **1**, and two areas of “steady state” could be seen in the temperature range 293–673 K, one at ca. 403 K, when the lattice ammonia is lost (97.2% expt; 97.7% theor), and one at ca. 673 K, after deammoniation when only one ammonia ligand or less is left (82.6% expt; 84.6% theor). The curve smoothly declines, and two ammonia ligands are lost, without distinctive plateaus (Figure S3 in the Supporting Information), leaving a complex with one ammonia molecule bound. Ag AAS analyses performed on ground **1** at ambient temperature are

(44) Bruker SMART and SAINT, area detector control and integration software; Bruker Analytical X-ray Systems: Madison, WI, 1995.

(45) Sheldrick, G. M. *Acta Crystallogr., Sect. A* **1990**, *46*, 467.

(46) Burges, C. W.; Koschmieder, R.; Sahn, W.; Schwenk, A. Z. *Naturforsch., A: Phys. Phys. Chem., Kosmophys.* **1973**, *28*, 1753.

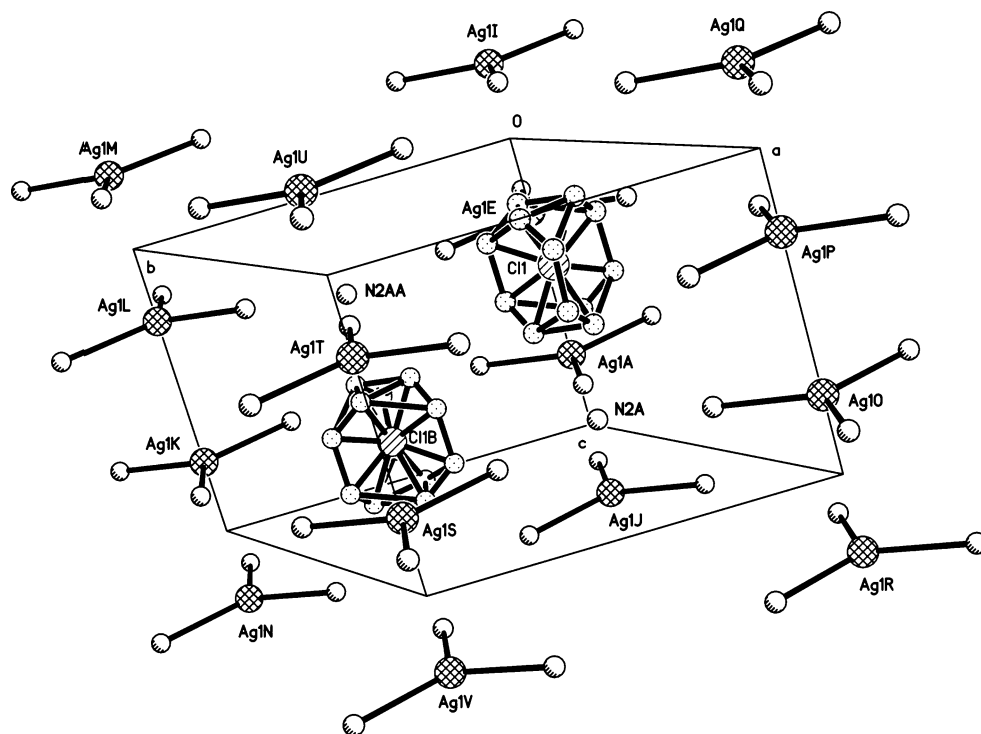


Figure 2. Crystal structure of **1**.

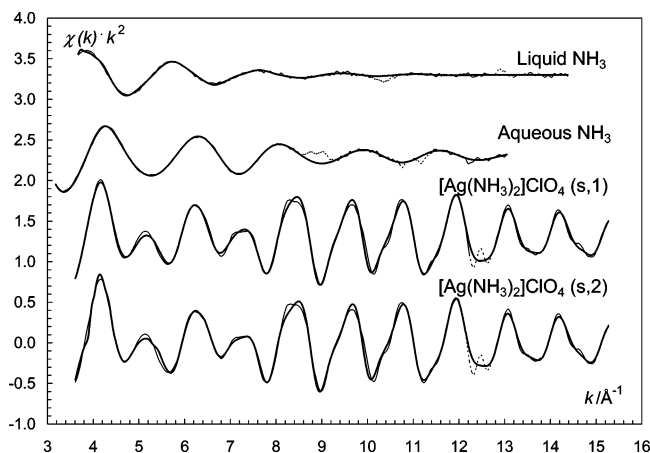


Figure 3. k^2 -weighted EXAFS data of experimental (thin line) and theoretical (thick line) data of the ammonia-solvated Ag^{I} ion in liquid and aqueous ammonia and of solid $[\text{Ag}(\text{NH}_3)_2]\text{ClO}_4$, formed after being heated to 333 K for 10 min (s1) and grinding at room temperature (s2). Data regions excluded in the refinements are shown with dotted thin lines in the experimental data.

in agreement with the composition of $[\text{Ag}(\text{NH}_3)_2]\text{ClO}_4$; silver content, 44.6% (expt), 44.7% (theor).

Ag^{I} in Liquid and Aqueous Ammonia. EXAFS data of liquid and aqueous ammonia solutions of silver(I) perchlorate (Figures 3 and S2 in the Supporting Information and Table 3) reveal that the ammonia-solvated Ag^{I} ion has different geometric arrangements in the two solvents. The mean Ag–N bond distance in aqueous ammonia ($\log [\text{NH}_3] = 1.12$; Figure 1) is much shorter than that in liquid ammonia, 2.15(1) and 2.26(1) Å, respectively, strongly indicating linear and trigonal configurations, respectively. The fit of the experimental data of the silver(I) perchlorate solution in liquid ammonia is improved by the introduction of a very long Ag–O distance. Ion-pair formation seems to take place

in liquid ammonia, most probably because of the low permittivity of the solvent, while the salts are completely dissociated in aqueous ammonia. The large Debye–Waller parameter of the trigonal $\text{Ag}(\text{NH}_3)_3^+$ complex in liquid ammonia may indicate that the complex has nonequidistant Ag–N bonds. The high symmetry of the trigonal $\text{Ag}(\text{NH}_3)_3^+$ complex in the solid state may be caused by a random distribution of distorted complexes in a way similar to that described for Cu^{II} complexes found to be regularly octahedral from crystallography.⁴⁷ The fairly long Ag–N bond distance of 2.22(2) Å in the linear $\text{Ag}(\text{NH}_3)_2^+$ complex in aqueous ammonia reported from a LAXS study¹⁷ could not be confirmed by EXAFS in this study. The Ag–N bond distance of 2.15(1) Å in the bisamminesilver(I) ion in an aqueous ammonia solution (Table 3) is within the range of distances found in the crystal structure determinations of the linear bisamminesilver(I) complexes (see Introduction). The mean Ag–N bond distance of 2.26(1) Å in liquid-ammonia-solvated trisamminesilver(I) is close to the one found in the crystal structures of $[\text{Ag}(\text{NH}_3)_3]\text{NO}_3$ ¹¹ and **1**; see Introduction and Table 3. Thus, the change in the mean coordination number when the Ag^{I} ion is transferred from aqueous to liquid ammonia is caused by an increased ammonia activity; see Figure 1. Theoretical studies of the ammonia-solvated Ag^{I} ion in silver(I)–ammonia clusters in the gaseous phase show a very fine balance between two- and three-coordinated species, with linear complexes somewhat more stable than the planar three-coordinated ones.⁴⁸ This is in contradiction to the results in this and previous studies when the ammonia activity is high; see Introduction.

(47) Fox, B. S.; Beyer, M. K.; Bondybej, V. E. *J. Am. Chem. Soc.* **2002**, *124*, 13613.

(48) Persson, I.; Persson, P.; Sandström, M.; Ullström, A.-S. *J. Chem. Soc., Dalton Trans.* **2002**, 1256.

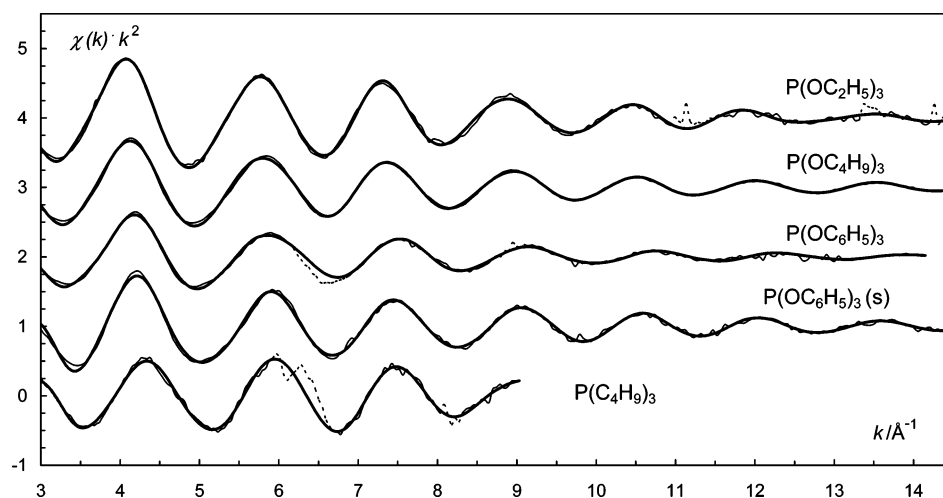


Figure 4. k^2 -weighted EXAFS data of experimental (thin line) and theoretical (thick line) data of the triethyl, tri-*n*-butyl and triphenyl phosphite, and tri-*n*-butylphosphine solvated Ag^{I} ions in solution. Data regions excluded in the refinements are shown with dotted thin lines in the experimental data.

Ag^{I} in Triethyl, Tri-*n*-butyl, and Triphenyl Phosphite and Tri-*n*-butylphosphine Solutions. The mean $\text{Ag}-\text{P}$ bond distances of 2.48–2.51 Å in the solvates of Ag^{I} in trialkyl and triphenyl phosphite solutions (Table 3) correspond to a trigonal configuration geometry around the Ag^{I} ion (see Introduction). The mean $\text{Ag}-\text{P}$ bond distance in tri-*n*-butylphosphine, 2.53(1) Å, is slightly longer than that in the phosphites. This longer $\text{Ag}-\text{P}$ bond distance is expected because the electron cloud on phosphines is slightly larger than that on phosphites because of the electron-withdrawing effects of the O atoms in phosphites. The $\text{Ag}-\text{P}-\text{O}$ angles are 112–116° for the phosphite silver(I) complexes, and the $\text{Ag}-\text{P}-\text{C}$ angle in the tris(tri-*n*-butylphosphine)silver(I) complex is ca. 110°. The fit of the experimental data of the silver(I) perchlorate solution in tri-*n*-butylphosphine is improved by the introduction of a very long $\text{Ag}-\text{O}$ distance. An ion-pair formation is not surprising in tri-*n*-butylphosphine because of its low permittivity. The structural parameters of the solvated Ag^{I} ions in trialkyl and triphenyl phosphite and tri-*n*-butylphosphine as determined by EXAFS are summarized in Table 3; the fits to the EXAFS data are given in Figure 4 and those of the Fourier transforms in Figure S2 in the Supporting Information.

Au^{I} in Liquid and Aqueous Ammonia. EXAFS data of **3** containing the bisamminegold(I) ion, $[\text{Au}(\text{NH}_3)_2]^+$, gives a $\text{Au}-\text{N}$ bond distance of 2.025(5) Å, and the $\text{Au}-\text{N}$ bond distances in the Au^{I} solvates in aqueous and liquid ammonia are 2.022(5) and 2.026(7) Å, respectively (Table 4). Consequently, the linear bisamminegold(I) ion is strongly predominating in both liquid and aqueous ammonia solutions and with the same $\text{Au}-\text{N}$ bond distance as that in solid $[\text{Au}(\text{NH}_3)_2]\text{Br}$.²⁹ The bisamminegold(I) solvate in a liquid ammonia solution has a $\text{N}-\text{Au}-\text{N}$ angle of 180.0(5)° (Table 4); the $\text{N}-\text{Au}-\text{N}$ angle is 178.7(8)° in $[\text{Au}(\text{NH}_3)_2]\text{Br}$ because of H bonds from the ammonia H atoms to the bromide ions.²⁹ In solid $[\text{Au}(\text{NH}_3)_2]\text{Br}$, there are also $\text{Au}-\text{Au}$ distances at 3.414(1) Å, but the EXAFS data on **3** reveal no such distances. The results are summarized in Table 4; the fittings of the EXAFS data are given in Figure 5, including the individual contributions in Figure S4 in the Supporting

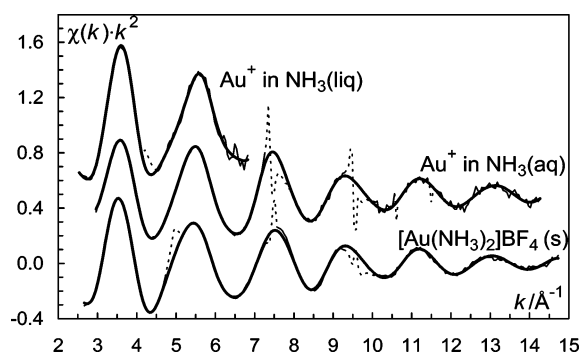


Figure 5. k^2 -weighted EXAFS data of experimental (thin line) and theoretical (thick line) data of the ammonia-solvated Au^{I} ion in liquid and aqueous ammonia and of solid $[\text{Au}(\text{NH}_3)_2]\text{BF}_4$. Data regions excluded in the refinements are shown with dotted thin lines in the experimental data.

Information, the fittings of the Fourier transforms are given in Figure S5 in the Supporting Information, and the absorption edges are given in Figure S6 in the Supporting Information. Attempts to perform single-crystal X-ray crystallography on **3** have been made before but failed because of photosensitive and unstable crystals.²⁹ The GNXAS program allows the omission of erroneous data points or data regions, e.g., due to glitches, in the refinements of structural parameters, and such data points cannot be deleted or replaced. These regions are marked with dots in the experimental data functions in Figures 5 and S4 in the Supporting Information.

Au^{I} in Triethyl Phosphite and Tri-*n*-butylphosphine Solutions. The mean $\text{Au}-\text{P}$ bond distances in the Au^{I} solvates of triethyl phosphite and tri-*n*-butylphosphine are 2.37(1) and 2.40(1) Å, respectively (Table 4 and Figures 6 and S5 in the Supporting Information). The mean $\text{Au}-\text{P}$ bond lengths fit very well with three-coordination (see Introduction), and the more expanded electron cloud on the phosphine than on the phosphite (see the Ag section above) explains the longer $\text{Au}-\text{P}$ bond distance in the phosphine. The $\text{Au}-\text{P}-\text{O}$ and $\text{Au}-\text{P}-\text{C}$ angles are both 115°.

Raman Spectroscopy of Ammonia-Solvated Ag^{I} and Au^{I} Ions. The wavenumbers recorded for the bisammine-silver(I) complex formed in an aqueous ammonia solution,

Table 5. Raman Bands and Assignments of the Ag^I and Au^I Complexes Formed in Aqueous and Liquid Ammonia, in the Solid State and Solution

sample	M-NH ₃	NO ₃ ⁻ /ClO ₄ ⁻ /BF ₄ ⁻			ammonia			
	ν_{sym}	ν_1	ν_4	ν_2	$\delta(\text{NH}_3)_{\text{deg}}$	$2\delta(\text{NH}_3)_{\text{deg}}$	$\nu(\text{NH}_3)_{\text{sym}}$	$\nu(\text{NH}_3)_{\text{as}}$
[Ag(NH ₃) ₂]ClO ₄ (s)	378	934	625	459	1611	3182	3292	3358
[Ag(NH ₃) ₂]NO ₃ in NH ₃ (aq)	370	1048	1616				3310	
[Ag(NH ₃) ₂]ClO ₄ in NH ₃ (l)	238	934	627	460	1636	3215	3300	3377
[Ag(NH ₃) ₃]NO ₃ in NH ₃ (l)	317	1044				3215	3298	3380
[Au(NH ₃) ₂]BF ₄ in NH ₃ (l)	385	920			1641	3215	3300	3381
NH ₃ (l)					1642	3215	3300	3381

and the degraded form [Ag(NH₃)₂]ClO₄ produced from liquid ammonia, are in agreement with a previous study of bisamminesilver(I) perchlorate in solution and bisamine-silver(I) nitrate in the solid state, with symmetric Ag-N stretching wavenumbers present at 369 and 372 cm⁻¹, respectively.⁴⁹ The spectrum of the linear bisamminesilver(I) ion in aqueous ammonia is not very well-resolved, and the corresponding stretching wavenumber is found, as in previous studies, at ca. 370 cm⁻¹.⁵⁰ The assignments of the recorded Raman wavenumbers are listed in Table 5. The results from the measurements of silver(I) nitrate in liquid ammonia show a weak Ag-N symmetric stretching wavenumber at ca. 317 cm⁻¹, close to the wavenumber reported by Lundeen and Tobias,⁵⁰ who curve-fitted their peak into two wavenumbers, 296 and 329 cm⁻¹. Gans and Gill reported a Ag-N symmetric stretching wavenumber of silver nitrate in liquid ammonia at 263 cm⁻¹.¹⁸ We have also studied a liquid ammonia solution of silver(I) perchlorate where a fairly strong band at 238 cm⁻¹ has been assigned to the Ag-N symmetric stretching wavenumber, for which the lower wavenumber may be an effect of the ion-pair formation mentioned above.

¹⁰⁷Ag NMR of Solvated Ag^I Ions. The ¹⁰⁷Ag NMR chemical shifts of a number of Ag^I solvates have been recorded in order to further characterize the Ag solvate complexes studied; the shifts are given relative to an intrinsic solution of silver nitrate in heavy water, D₂O (Figure 7). Because the change in shift is rather large between various Ag^I solvates, the difference depends on the environment of the Ag nucleus. The largest shielding is observed in the solvates with the strongest Ag-solvate bonds, the most bulky solvent molecules, and high coordination number. There is a significant shift of the ammonia-solvated Ag^I ions in aqueous and liquid ammonia. Because the shift is dependent on the concentration of the Ag^I ions,⁵¹ three different concentrations of silver nitrate in aqueous ammonia, 0.44–6.0 mol·dm⁻³, were measured. However, the range in shift is narrow, 430–450 ppm, and the difference is not large enough to intervene with shifts of Ag^I in other solvents. Because the ¹⁰⁷Ag NMR shift is also dependent on the anion, both silver nitrate and silver perchlorate in liquid ammonia were investigated. The difference in the shift of 0.44 mol·dm⁻³ solutions was negligible.

(49) Miles, M. G.; Patterson, J. H.; Hobbs, C. W.; Hopper, M. J.; Overend, J.; Tobias, R. S. *Inorg. Chem.* **1968**, *7*, 1721.

(50) Lundeen, J. W.; Tobias, R. S. *J. Chem. Phys.* **1975**, *63*, 924.

(51) Jucker, K.; Sahm, W.; Schwenk, A. *Z. Naturforsch. A: Phys., Phys. Chem., Kosmophys.* **1976**, *31*, 1532.

(52) Lamble, G.; Moen, A.; Nicholson, D. *J. Chem. Soc., Faraday Trans.* **1994**, *90*, 2211.

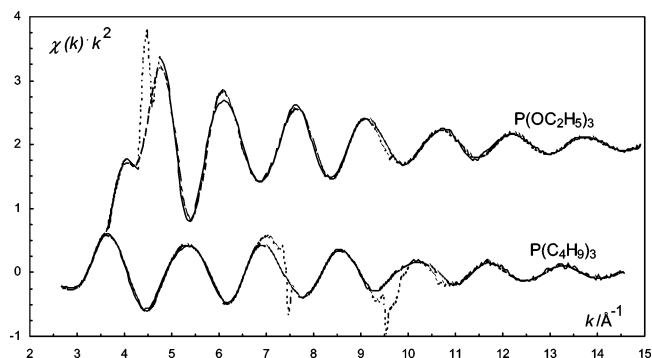


Figure 6. k^2 -weighted EXAFS data of experimental (solid) and theoretical (dashed) data of the triethyl phosphite and tri-*n*-butylphosphine solvated Au^I ions in solution.

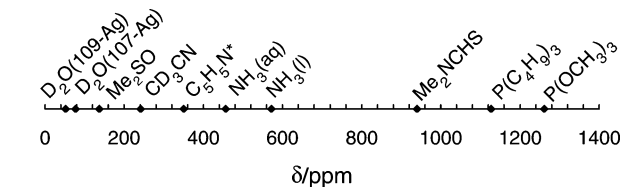


Figure 7. ¹⁰⁷Ag NMR shifts of the solvated Ag^I ion in different solvents. *¹⁰⁹Ag measurement in ref 57.

Coordination Chemistry of the Monovalent Group 11 Metal Ions in Soft Donor Solvents. The coordination chemistry of the monovalent group 11 metal ions in the solvents with the strongest electron-pair donor properties, liquid and aqueous ammonia, trialkyl and triaryl phosphites, and trialkyl- and triarylphosphines, shows that the maximum allowed coordination numbers possible are not observed in solution but sometimes in the solid state (Table 6).

The ammonia-solvated Cu^I, Ag^I, and Au^I ions are all linear in aqueous solution, while a trigonal configuration is observed in liquid ammonia for Cu^I and Ag^I because of higher ammonia activity; the linear configuration of bisamminegold(I) is so stable that any higher complexes are not formed, even in neat liquid ammonia.

Triarylphosphine complexes of Cu^I, Ag^I, and Au^I in linear, trigonal, and tetrahedral configurations are reported in the solid state (Table 6). Linear and tetrahedral copper(I) trialkylphosphine complexes are reported in the solid state, while for Ag^I only linear and for Au^I only linear and triangular trialkylphosphine complexes are reported so far (Table 6). The M-P bond distances in the tetrahedral triarylphosphine complexes are much longer than those in the corresponding trialkylphosphine complexes and are comparable to the corresponding linear and trigonal triarylphosphine complexes. This is certainly due to the large cone angle of triphenylphosphine (145°),⁵³ which causes the M-P bond distance to be largely controlled by the ligand-

Table 6. Summary of Mean M–L Bond Distances (in Å) in Solvate Complexes of the Monovalent Group 11 Metal Ions and the Strong Electron-Pair Donor Solvents Ammonia, Triaryl and Trialkyl Phosphite, and Triaryl- and Trialkylphosphine in the Solid State and in the Neat Solvent (Italics) in Basically Linear (2), Trigonal (3), and Tetrahedral (4) Configuration

	CN = 2	CN = 3	CN = 2		CN = 3		CN = 4		CN = 3		CN = 4
	NH ₃	NH ₃	PØ ₃	PR ₃	PØ ₃	PR ₃	PØ ₃	PR ₃	P(OØ) ₃	P(OR) ₃	P(OR) ₃
Cu ⁺	1.963/3 ^a <i>1.88^{b,c}</i>	N/A <i>2.00^{d,e}</i>	2.228/1 ^a	2.201/4 ^a	2.294/8 ^a	N/A	2.564/2 ^a	2.271/11 ^a	N/A	N/A	2.242/1 ^a
Ag ⁺	2.132/15 ^a <i>2.148^{b,d}</i>	2.272/1 ^{a,f} <i>2.26^{d,e}</i>	2.433/8 ^a	2.385/3 ^a	2.525/4 ^a	N/A <i>2.528^d</i>	2.649/12 ^a	N/A	2.481 ^g <i>2.485^d</i>	N/A	N/A
Au ⁺	2.020/1 ^{a,d} <i>2.025^{b,d,e}</i>	N/A	2.308/15 ^a	2.311/20 ^a	2.387/8 ^a	2.421/1 ^a <i>2.399^d</i>	2.533/2 ^c	N/A	N/A <i>2.367^d</i>	N/A	N/A

^a Number of solid-state structures in the mean value; see the Supporting Information for details. ^b Aqueous ammonia. ^c Reference 52. ^d This work, EXAFS data. ^e Liquid ammonia. ^f Mean of the results from ref 11 and 1. ^g Mean of the results from refs 21c and 21d. ^h Mean of the results from the triethyl and tri-*n*-butyl phosphite solutions.

ligand repulsion. The tri-*n*-alkylphosphine ligands have smaller cone angles and the alkyl groups are less space demanding than the phenyl groups, and any steric restrictions at the coordination of four ligands around the group 11 metal ions seem not to exist. On the other hand, tricyclohexylphosphine and trialkylphosphines with large branched alkyl chains have larger cone angles than triphenylphosphine and are thereby even more space-demanding.

The relativistic effects of especially Au^I causes that the size of the monovalent group 11 ion to increase in the order Cu⁺ < Au⁺ < Ag⁺ in steps of ca. 0.1 Å (Table 6).^{54,55} The coordination numbers of the solvate complexes in solution (neat solvents) are lower than those geometrically possible. This shows that the configuration is largely controlled by the molecule orbitals on the metal ions in solvate complexes dominated by covalent metal–ligand bonds.

Acknowledgment. We are grateful for the support from Rolf Andersson for the recording of Ag NMR data, from Dr. Mats Johnsson, Stockholm University, for carrying out

(53) Tolman, C. A. *Chem. Rev.* **1977**, *77*, 313.

(54) Ahrland, S.; Nilsson, K.; Persson, I.; Yuchi, A.; Penner-Hahn, J. E. *Inorg. Chem.* **1989**, *28*, 1833.

(55) Bayler, A.; Schier, A.; Bowmaker, G. A.; Schmidbaur, H. *J. Am. Chem. Soc.* **1996**, *118*, 7006.

the TGAs, and from Prof. Bo Liedberg, Department of Physics and Measurements, Linköping University, for the use of the Raman and IR spectrometers. We gratefully acknowledge the financial support given to these investigations by the Swedish Research Council. SSRL is gratefully acknowledged for allocation of beam time and laboratory facilities at our disposal. SSRL is operated by the Department of Energy, Office of Basic Energy Sciences. The SSRL Biotechnology Program is supported by the National Institutes of Health, National Center for Research Resources, Biomedical Technology Program, and by the Department of Energy, Office of Biological and Environmental Research.

Supporting Information Available: ¹⁰⁷Ag NMR shifts of Ag^I solvates in solution, TGA raw data, normalized XANES spectra of studied Ag^I and Au^I complexes, Fourier transforms of Ag^I and Au^I complexes, EXAFS data of Au^I complexes analyzed with the GNXAS program package, and a summary of the solid-state structures containing ammonia, trialkyl- and triarylphosphine, and trialkyl and triaryl phosphite solvated Cu^I, Ag^I, and Au^I ions. The reference manual to Table 6 is given in Tables S2–S4 including mean bond distances and references. This material is available free of charge via the Internet at <http://pubs.acs.org>.

IC060175V